The Photogrammetric Record 22(120): 290–308 (December 2007)

IMPORTANT CONSIDERATIONS FOR CRANIOFACIAL MAPPING USING LASER SCANNERS

ZULKEPLI MAJID (zulkepli@fksg.utm.my)
Universiti Teknologi Malaysia

ALBERT K. CHONG (chonga@albers.otago.ac.nz)
University of Otago, New Zealand

HALIM SETAN (halim@fksg.utm.my)
Universiti Teknologi Malaysia

Abstract

The use of a laser scanning system for human craniofacial mapping has gained considerable interest recently as it offers a non-contact method which is very efficient in capturing a vast amount of accurate spatial data. Nonetheless, there is a need for a thorough evaluation to identify the important technical factors which may affect the accuracy of the system. This paper discusses the tests and the results of an evaluation of the Minolta VI-910 3D laser scanning system used to capture craniofacial surface data. The research shows that the factors to consider for craniofacial mapping are: scan distance, camera focal length, laser beam intensity, scanning resolution, convergence angle and number of overlapping scans.

KEYWORDS: convergence angle, craniofacial mapping, focal length, laser scanner, scan beam intensity, scan resolution

INTRODUCTION

RESEARCH CARRIED OUT by Kusnoto and Evans (2002), Da Silveira et al. (2003) and Boehnen and Flynn (2005) to study 3D laser scanning technology for capturing 3D craniofacial soft-tissue data to model human faces has highlighted the efficiency of the technology. In general, the Konica Minolta VI-910 laser scanner was regarded as the most accurate scanner for the task (Fig. 1). The quality of the detail of the scan is significantly higher than other scanners which have been tested and this is an important advantage for biometrics and biomedical mapping (Kau et al., 2004; Majid et al., 2004; Kovacs et al., 2006). A drawback of the Minolta VI-910 laser scanner was that it took about 19 s to perform an accurate scan. The amount of time was considered too long and could cause error due to the subject's facial movement during scanning. To reduce the possibility of movement occurring between set-ups (one set-up for the left face scan and one for the right face scan) for a complete scan, two Minolta VI-910 laser scanners were acquired and they would be used simultaneously in the Malaysian national craniofacial mapping project which requires a linear measurement accuracy of 0·7 mm between pairs of landmarks.

The scanner exploits a technique known as structured light triangulation (Majid et al., 2004). The surface of the object is illuminated with a red laser beam. Assuming that the light is

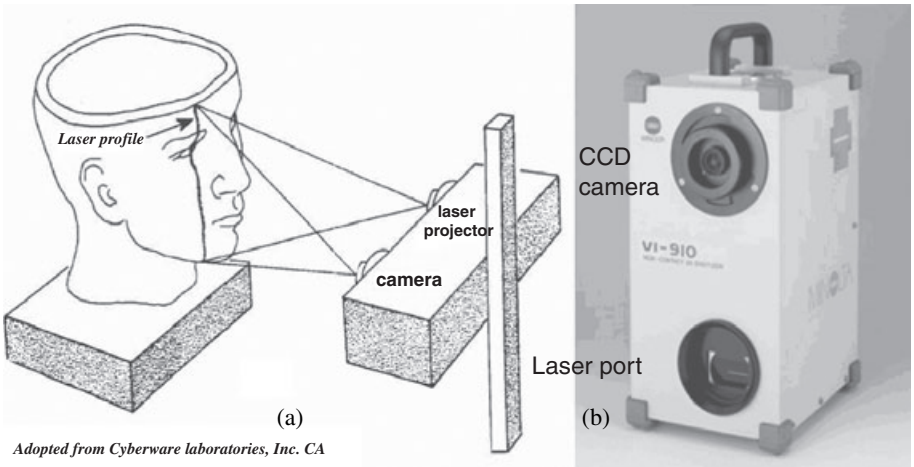

FIG. 1. Principle of laser scanner: (a) CCD camera and laser projector configuration; (b) Minolta VI-910.

projected in a single plane, a triangulation algorithm can determine the depth of the surface (Fig. 1(a)). Details of the mathematics can be obtained in Boyer and Kak (1987) and Sanderson et al. (1988). Generally, the system consists of a structured laser light source, a light projection system and a digital imaging system. The structured laser beam creates an ultra-thin profile on the object, which is photographed by a CCD camera mounted close to the projector. The relative position (a vector) between the internal reference point of the projection system and the camera lens is fixed. In addition, the angle of each projected laser profile plane and the angle of the camera optical axis are calibrated in advance. Subsequently, the x, y and z coordinates of the object-space position of each pixel on the object can be computed using the scale of the photography, the relative positional vector and the known angles. A least squares technique is used to compute a set of optimum 3D coordinates of the object surface.

This paper discusses the detail of the tests and results of studying the Minolta VI-910 laser scanner based on a few important technical factors considered to affect the accuracy for human craniofacial mapping. Details of each factor are provided in the sub-sections. The factors considered were as follows:

(1) scan distance (S_d) and camera focal length (f);
(2) scan resolution (R);
(3) scan intensity (I);
(4) number of overlapping scans per craniofacial area (N); and
(5) convergence angle (α).

It should be noted that these factors were studied separately. The interaction of these factors as a whole is beyond the scope of this study.

METHODOLOGY

Tests were carried out using a custom-built "bench-top-frame" device (Konica Minolta, Japan, Fig. 2). The VI-910 laser scanner was positioned as shown in the figure while the mannequin could be moved forward and/or backward using a sliding plate along a set of steel rails. Various scan distances could be set up for the test.

FIG. 2. Set-up of the tests using a custom-built device.

Test 1: Optimal Scan Distance and Camera Focal Length

The objective of the study was to find the optimal scan distance (distance from laser scanner to the subject) for scanning the human craniofacial area. The study also investigated which of the available lenses is most suitable for this application. The Minolta VI-910 scanner provides three types of lens: namely, wide angle ($f = 8$ mm); medium angle ($f = 14$ mm); and telephoto ($f = 25$ mm). A range of scan distances was used: 700, 800, 900 and 1000 mm. The scan distances were based on the findings of previous work on human craniofacial mapping conducted by the authors (Majid et al., 2005). A minimum scan distance of 700 mm was needed to cover the scan area using the medium-angle lens. Only the wide-angle lens and medium-angle lens were used in the tests. The telephoto lens was not selected because it is generally used for scanning small objects, such as a dental cast, and then often at a very short scan distance. According to the manufacturer, the telephoto lens could be used to scan a bigger object, but that would require long scan distances (>1000 mm) to obtain optimal coverage of the craniofacial area.

To mimic a human craniofacial object, a mannequin was marked with 1·5 mm diameter black circular dots representing craniofacial landmarks. Accordingly, the dot would return a 34-pixel sample at high and medium scanning resolution and an 8-pixel sample at low scanning resolution. Three sets of scans were performed for each scan distance, and for each set the mannequin was rotated 45° to the left and right as well as facing straight ahead (0°), so that a complete model of the craniofacial area could be obtained (Fig. 3). Subsequently, three sets of the 3D surface model of the mannequin were generated by precise registration and the merging process of each set of three scans using Rapidform 2004 software (version: PP2, INUS Technology, Seoul, South Korea). The software uses a set of proprietary algorithms in

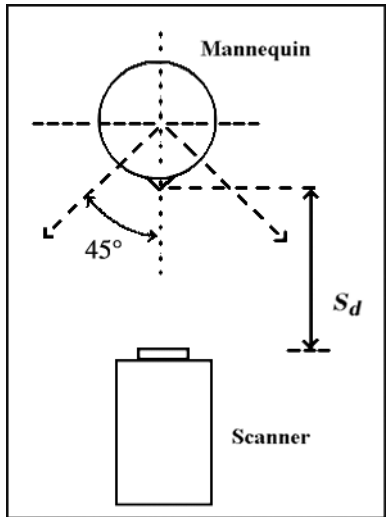

FIG. 3. Set-up of the scan distance test. Note that S_d is scan distance.

the merging process (including target centre determination), however, the authors believe that comparable techniques can be found in Haar et al. (2005). The registration and merging process of the software is as follows:

(a) Initial Registration. The initial registration roughly registers one scan (shell) with another overlapping one using geometric features on two scans (shells). Common geometric features, also known as corresponding points, are selected by the user. The accuracy of the initial registration was based on the accuracy of pairs of the corresponding points selected by the user. The more accurately the corresponding points are located, the better the registration result. For good accuracy, the number of selected pairs of corresponding points is between five and eight.

(b) Fine Registration and Merging Process. The fine registration process matches the overlapped regions of all the selected shells (in this case there are two: left scan from left scanner and right scan from right scanner). The merging process combines the data of the overlapping areas into a single point set. After merging, the difference between the data-sets is displayed as shell–shell deviation. The deviations between the surfaces were computed by using the normal from one of the surfaces to the other.

Consequently, the shell–shell deviation technique is an analysis of the quality of the registration of two adjacent overlapping scans. The technique may be used to evaluate the closeness of fit of two similar 3D surfaces (obtained from different viewpoints or different epochs) of the same object.

Slope distances (the shortest distance between two points in space) between the landmarks were measured using the ''point to point measure'' function of the same software. These distances were compared to the slope distance obtained by the Microscribe 3D digitiser system, which has a reported accuracy of 0·23 mm (Immersion Corporation, San José, CA, USA). The calibration of the Microscribe digitiser is not discussed in this paper, however, detailed information may be found from many sources such as Farag and Eid (2003) and Autodessys Inc. (2004).

Test 2: Laser Intensity

The maximum power of the laser was considered eye-safe by the manufacturer. The intensity of the scan beam can be set to auto mode or the user can adjust the beam manually. The main concern was the effect of the beam's intensity on the accuracy of the scanned data. By observing the laser beam of various intensities (numerical value on display) the "blooming" effect of the beam can be seen (Atkinson, 1996). A higher beam intensity causes higher backscattering, resulting in the phenomenon of blooming. Consequently, the beam intensity may have adverse effects on the texture and accuracy of the captured 3D spatial data. The test was designed to determine the optimal intensity of the laser beam required to obtain high quality data (spatial and texture) of the craniofacial surface. A mannequin textured so as to resemble human skin was selected for the test. The mannequin was scanned at various laser intensity values as shown in Fig. 4. All scans of this test were conducted at the same scan distance. The optimum scan distance obtained in Test 1 was used here. Similar to the previous test, the slope distances obtained from the test were compared with the distances gained from the Microscribe 3D digitiser system.

Test 3: Scanning Resolution

The Minolta VI-910 3D digitiser provides three classes of scanning resolution, namely: (1) low resolution (fast mode); (2) medium resolution (fine mode with one scan); and (3) high resolution (fine mode with three repeated scans). These scanning modes produce a different density of 3D point clouds and a different texture resolution. Tests were carried out using the three scanning modes to scan the craniofacial area of the mannequin and the process was repeated twice to ensure high quality data was captured for analysis. More details of the characteristics of point cloud intensity and the texture difference for the three scan resolutions are provided in the results and analyses section.

Test 4: Number of Overlapping Scans for the Craniofacial Area

The purpose of the test was to determine the optimal number of overlapping scans required to obtain a high quality complete 3D surface model of the craniofacial area. In general, a complete 3D model of the craniofacial area covers the surface from the left ear to the right ear and from the hairline to the bottom part of the chin. To obtain a complete surface model of the craniofacial area, the number of overlapping scans was considered an important

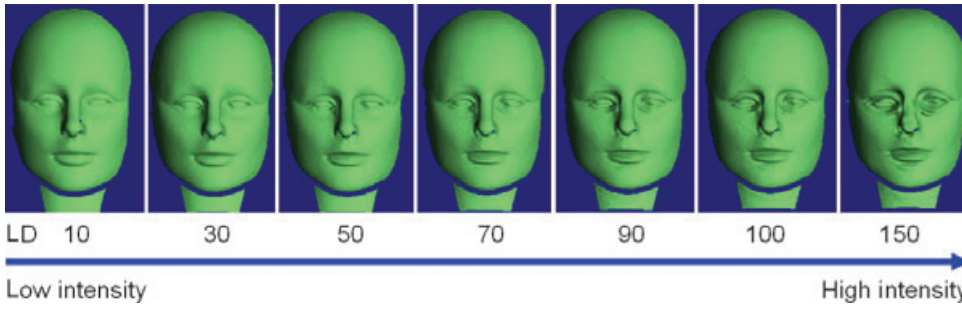

FIG. 4. Laser intensity in numerical values. Note the level of shading just below the right eye as laser intensity increases.

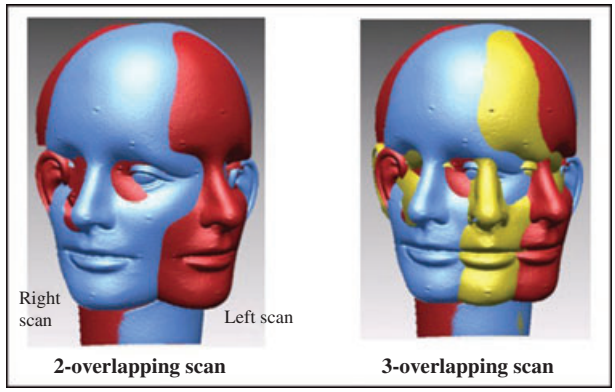

FIG. 5. Two and three overlapping scan configurations.

factor for both efficiency and accuracy. The test involved the acquisition of two sets of scans as described below (Fig. 5):

(1) three overlapping scans: the front view, the left and the right views of the mannequin;
(2) two overlapping scans: the left and the right views of the mannequin.

Overlapping scans were registered and merged to obtain a complete surface of the craniofacial area using Rapidform software (PP2). The evaluation of the test involved the measurements between craniofacial landmarks, marked as black dots on the mannequin. The slope distances obtained from the test were compared with the distances gained from the Microscribe 3D digitiser system.

Test 5: Convergence Angle

The test determined the optimal convergence angle (α) for setting the scanners to capture the craniofacial area (Fig. 6). The convergence angle is defined as twice ($2\times$) the angle

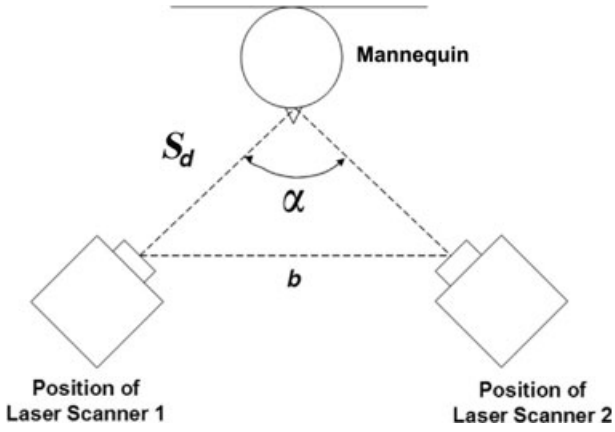

FIG. 6. The set-up for evaluating the convergence angle (α).

subtended between the vertical plane bisecting the head along the nose and the optical axis of the scanner camera lens. A set of convergence angles ranging from 20° to 140° at 20° intervals was used. In addition, the scan distance was fixed at 700 mm (based on previous test results of Test 1). Also, the aim of the study was to determine the optical geometry of the camera which would give the best results when two scanners were used together. The optical geometry could be a representation of the base (b) and S_d or α as shown in Fig. 6.

The scans from both scanners for each test angle were registered and merged using the Rapidform software. Again, slope distances of the landmarks were compared to the ''true'' slope distance. In addition, the accuracy of the merged data captured at each convergence angle was evaluated using the shell–shell deviation method.

RESULTS AND ANALYSES

Test 1: Optimal Scan Distance and Camera Focal Length

The slope distances between selected landmarks were determined by the Microscribe 3D digitiser system and the average of five sets was used as the ''true'' slope distance (Fig. 7). The same slope distances measured on the 3D craniofacial surface model were compared with the ''true value''.

Tables I and II show the results of the medium-angle lens and the wide-angle lens tests, respectively. The scan distances (S_d in mm) are shown at the top of the tables and all measurements are in millimetres. Only seven important slope distances were selected from a set of several hundred combinations. They are the distances normally required for anthropometric study.

The differences between the measurement of the Microscribe 3D digitiser and the wide-angle measurements shown in Table II are positive, indicating the possibility of a bias or scale error. Further analysis shows that the values are within the manufacturers' specifications for both systems and hence no further analysis was carried out on the results. In the context of this paper, the standard deviation is more important than the mean error as the project specifications

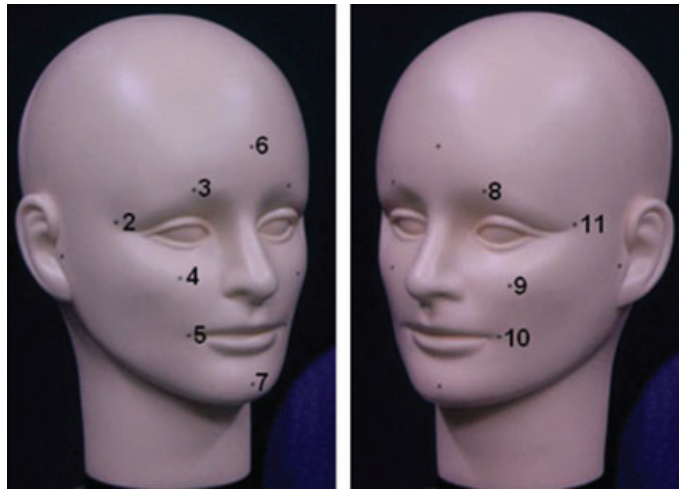

FIG. 7. The location of the anthropometric marks discussed in the paper.

TABLE I. Slope distance comparison of the medium-angle lens measurement of various scan distances. Note that the true values and the measurements are in the Appendix.

From–To	$S_d = 700$	$S_d = 800$	$S_d = 900$	$S_d = 1000$
3–8	−0·063	−0·011	0·642	0·514
4–9	−0·249	0·825	0·978	0·83
5–10	−0·084	−0·309	1·186	0·238
6–7	0·112	0·709	1·57	0·904
3–4	−0·019	0·64	0·422	0·283
8–9	−0·12	0·569	0·677	0·411
2–11	−0·388	0·548	2·205	2·193
Mean	−0·116	0·424	1·097	0·768
Standard deviation	0·162	0·419	0·621	0·678

TABLE II. Slope distance comparison of the wide-angle lens measurement of various scan distances.

From–To	$S_d = 700$	$S_d = 800$	$S_d = 900$	$S_d = 1000$
3–8	1·632	1·554	0·871	1·082
4–9	2·501	1·645	1·613	1·541
5–10	2·076	1·618	1·458	1·027
6–7	4·075	3·64	2·948	3·042
3–4	2·115	1·629	1·687	1·695
8–9	1·6	0·995	1·537	1·54
2–11	4·116	3·854	3·716	2·44
Mean	2·588	2·134	1·976	1·767
Standard deviation	1·075	1·127	0·989	0·731

provide for the value of measurement standard deviation. Further analyses are provided in the discussion section.

In general the results show that the medium-angle lens gives the best values for all scan distances tested. Nevertheless, the results also show that the accuracy reduces as the scan distance increases.

Test 2: Laser Intensity

Fig. 8 shows: (a) the true shape and colour of the mannequin's right eye (picture taken by a digital camera); and (b) the surface shown in (a) darkens as the beam intensity increases. Fig. 9 shows: (a) the shape of the nose worsens as the intensity increases; (b) the amount of shape change between intensity value of 20 to intensity value of 220; and (c) the shape change in (b) as depicted by the grid mesh. In short, the figure shows that adjusting the beam intensity manually could introduce large errors in the scan. Consequently, the use of the manual setting should be carried out with caution. The Minolta VI-910 3D laser scanner is an intelligent scanner; a built-in sensor determines the optimal laser intensity required at a set scan distance. Fig. 10 shows the error in the shell–shell deviation between a surface model scanned at the optimal laser intensity (around 20 to 40) and one scanned at an intensity of 150. Fig. 11 shows the average shell–shell rms deviation versus the laser intensity. In addition, Table III shows a sample of the results of slope distance comparisons. They are: (1) scan at intensity value 20; (2) scan at intensity value 100; and (3) scan at intensity value 150. More discussion can be found in the discussion section of this paper.

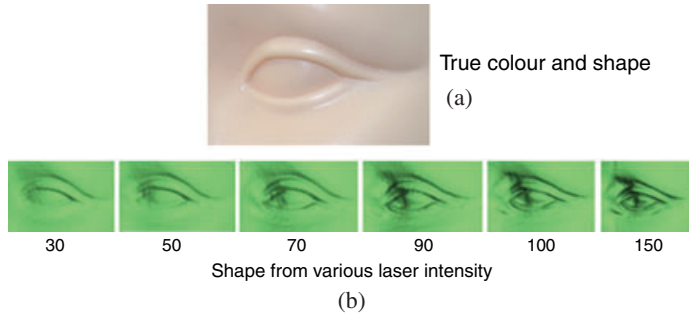

FIG. 8. Texture quality versus laser beam intensity: (a) true colour; (b) shape obscured due to increased beam intensity.

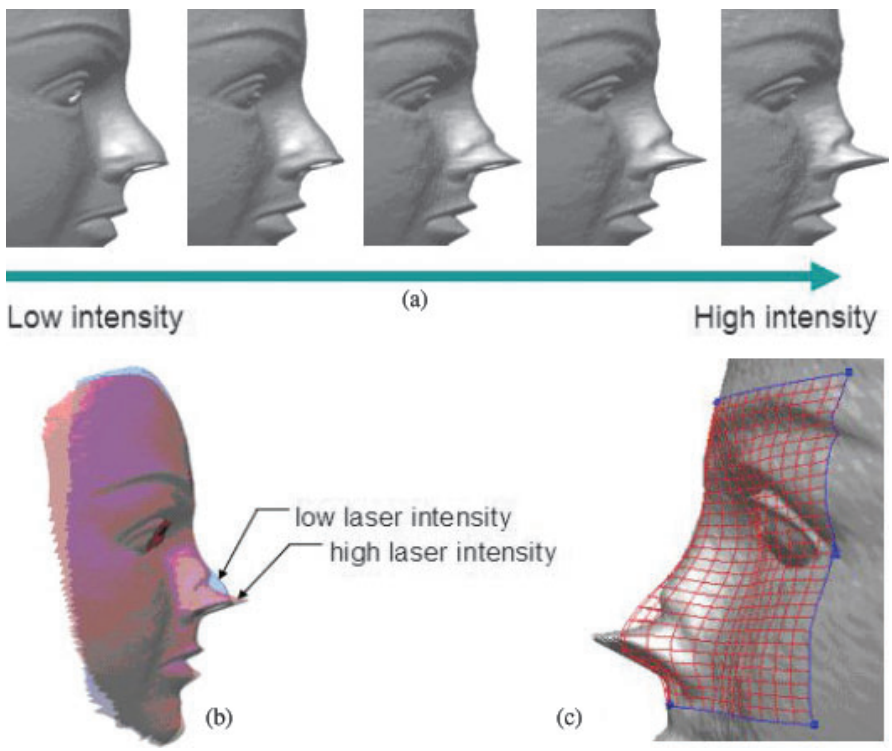

FIG. 9. Scan error versus beam intensity: (a) shape change based on intensity; (b) surface shape change introduced; (c) the shape change of (b) as depicted by a grid mesh.

Test 3: Scanning Resolution

The shell–shell deviation analysis was carried out to find the maximum deviation value between (a) low–high resolution data-sets and (b) medium–high resolution data-sets. The results of the study are presented in Table IV.

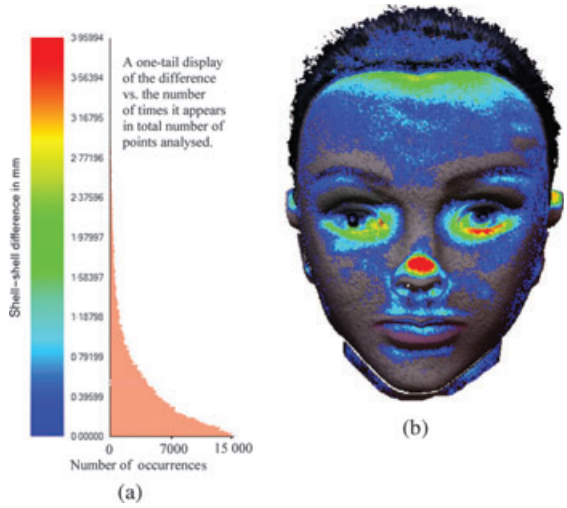

FIG. 10. Shell–shell deviation analysis: (a) a normal distribution of shell–shell difference in mm; (b) the location of large differences as depicted by bright colours.

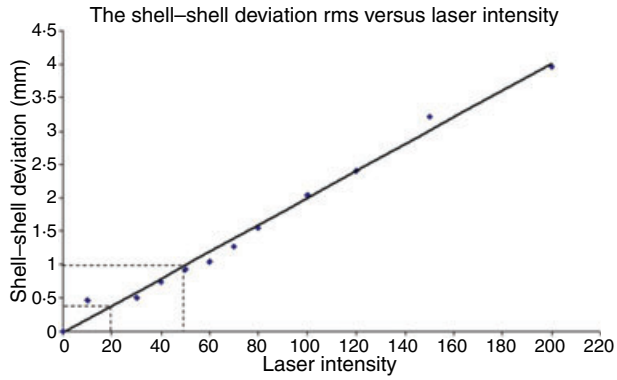

FIG. 11. A graph showing the averaged shell–shell rms deviation versus the laser intensity value. Note that the optimal intensity lies between the dotted lines.

TABLE III. A sample of the slope distance comparison of the beam intensity test results.

From–To	*At I = 20 (mm)*	*At I = 100 (mm)*	*At I = 150 (mm)*
3–8	−0·202	−0·327	−0·341
4–9	0·056	0·239	−0·459
5–10	0·005	0·279	−0·246
6–7	0·552	2·973	2·406
3–4	−0·09	1·216	1·247
8–9	−0·012	0·191	0·871
2–11	0·589	1·025	1·003
Mean	0·128	0·799	0·640
Std deviation	0·290	1·012	0·973

TABLE IV. Shell–shell deviation analysis of scanning resolution.

Resolution test	*Maximum deviation (mm)*	*Average deviation (mm)*	*Standard deviation (mm)*
Low–High	1·065	0·446	0·215
Medium–High	0·349	0·040	0·047

The table shows that the scanning resolutions suitable for the craniofacial surface are the high and medium resolutions with maximum shell–shell deviation of 0·349 mm compared to low resolution of 1·065. Additionally, the test results show that both high and medium resolution scans have a similar point density of 576 per square inch (0·044 mm pixel^{-1}), however, the low resolution produces only 144 per square inch. Fig. 12 shows the distribution of points in the point cloud. Table V shows the results of slope distance comparison and the standard deviation indicates that both medium and high resolution scans are suitable for this project.

Test 4: Number of Overlapping Scans Needed for the Craniofacial Area

The results of the slope distance comparison between the "true", two-scan and three-scan configuration shows that the best measurement belongs to the three-scan configuration (Table VI). However, the two-scan configuration gave a standard deviation of 0·632 mm which satisfies the landmark measurement accuracy of 0·7 mm for this craniofacial project. In general, a three-scan configuration would require the use of three scanners as head movement could produce large errors in the data-set when all three scans were not carried out simultaneously.

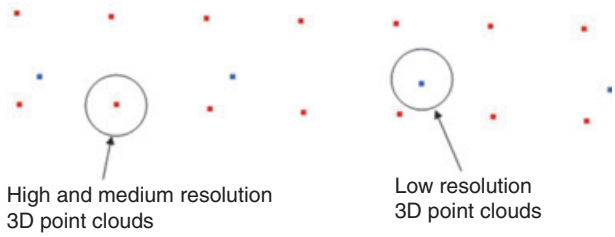

FIG. 12. Point cloud density based on scanning resolution.

TABLE V. Slope distance comparison of the scanning resolution test.

From–To	*Low resolution (mm)*	*Medium resolution (mm)*	*High resolution (mm)*
3–8	−0·553	−0·727	−0·515
4–9	−0·052	−0·104	0·168
5–10	−0·322	−0·586	−0·658
6–7	2·318	0·168	−0·176
3–4	1·195	0·464	0·767
8–9	1·023	0·261	0·692
2–11	0·444	0·731	0·973
Mean	0·579	0·03	0·179
Std deviation	0·934	0·496	0·603

TABLE VI. Slope distance comparison between the 'true' value, 2-scan and 3-scan measurement.

From–To	*True value (mm) (A)*	*2 scans test (mm) (B)*	*3 scans test (mm) (C)*	*B-A*	*C-A*
3–8	52·959	52·867	52·939	−0·092	−0·02
4–9	61·387	61·040	61·551	−0·347	0·164
5–10	57·745	57·150	57·672	−0·595	−0·073
6–7	115·239	115·826	115·577	0·587	0·338
3–4	46·573	47·192	47·196	0·619	0·623
8–9	47·705	48·202	48·143	0·497	0·438
2–11	112·505	113·547	113·483	1·042	0·978
			Mean	0·244	0·349
			Std deviation	0·551	0·344

Test 5: Convergence Angle

In the data analysis, slope distances between landmarks were compared to the "true" value. In addition, the registration accuracy of each convergence angle was evaluated using the shell-to-shell deviation method.

Fig. 13 shows the size of the overlapping area in relationship to the convergence angle and Table VII shows the approximate percentage of overlap over the craniofacial area. In Fig. 14 it can be seen that the shell–shell deviation error at the 90° convergence angle is smaller, compared to other convergence angles. The test also involved larger convergence

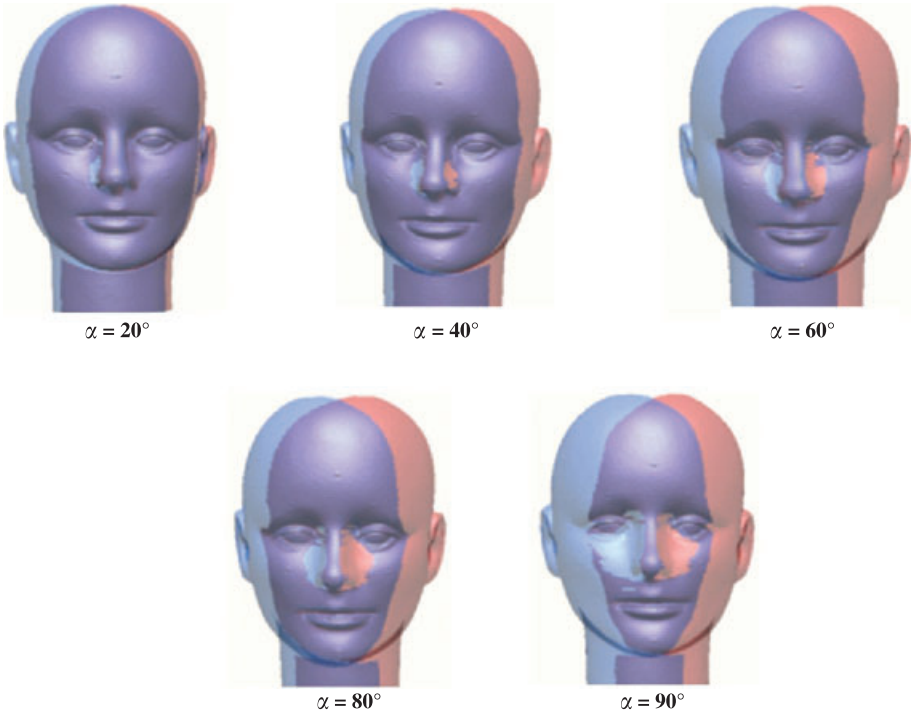

FIG. 13. The effect of the convergence angle on the corresponding overlapping area.

TABLE VII. Approximate percentage of overlap of the figure shown in Fig. 13.

Convergence angle	$\alpha = 20$	$\alpha = 40$	$\alpha = 60$	$\alpha = 80$	$\alpha = 90$
Percentage (%)	89	85	81	77	72

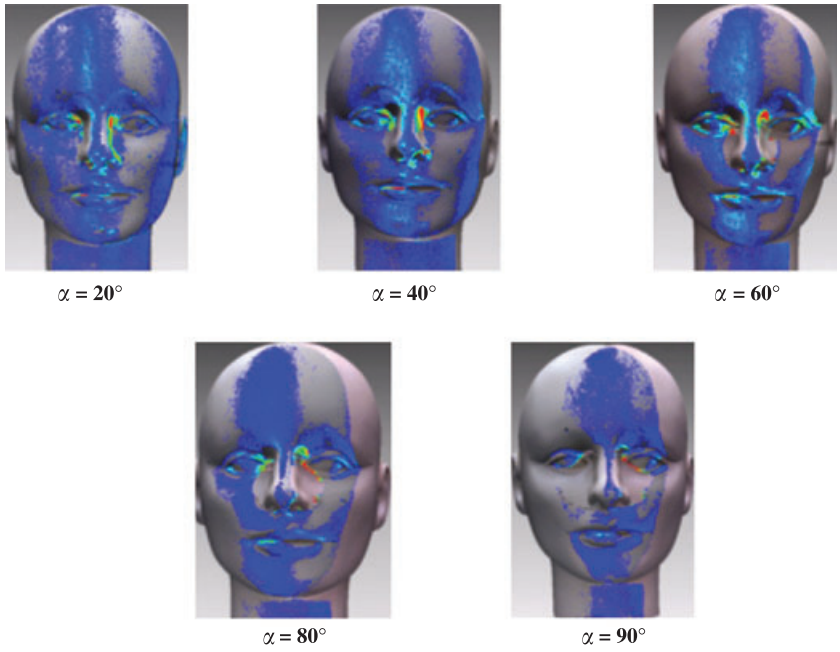

FIG. 14. Shell–shell deviation analysis of the convergence angle test. Note that the colour chart used is similar to that in Fig. 10.

angles (120° and 140°); however, the registration failed (Fig. 15) because of the limited number of available corresponding features to perform high quality registration (Fig. 16).

The test on the optimal convergence angle was evaluated by analysing completeness of the 3D model that covered the craniofacial area (from the left ear to the right ear, from the hairline to the bottom of the chin). Fig. 17 shows the effect of the convergence angle on the shape of the modelled mannequin's ear. The figure shows clearly that the shape of the inner loop of the modelled ear becomes smoother as the angle increases. It seems that the closer the convergence angle is to the normal to the plane of the ear the more accurate the scan data which could be obtained. More information is provided in the discussion section. Table VIII shows the results of the slope distance comparison of the convergence angle test. The standard deviations obtained for the convergence angles 60°, 80° and 90° satisfy the project accuracy requirement.

DISCUSSION

Accuracy Factor

Generally, for a typical single scan the accuracy of the 3D points is comparable to the value provided by the manufacturer. In this study of craniofacial mapping, initial tests showed

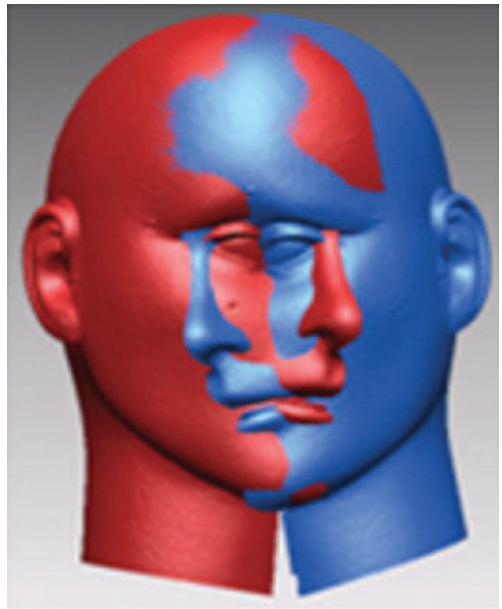

FIG. 15. Errors in the registration of the left and right scans of the 120° convergence angle.

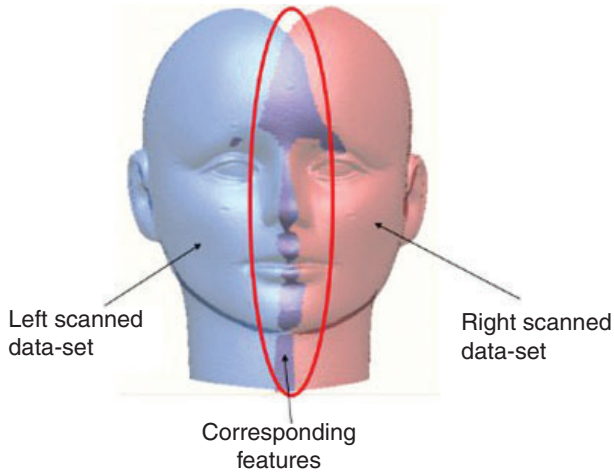

FIG. 16. Limited number of corresponding features to perform accurate 3D registration of the two overlapping scans.

that there might be factors which could influence the quality of the captured data. Consequently, it was apparent that the accuracy of the laser scanning system for craniofacial mapping is a function of several parameters such as scan distance, focal length of lens, scanning resolution, laser beam intensity and the number of scans. Equation (1) expresses the

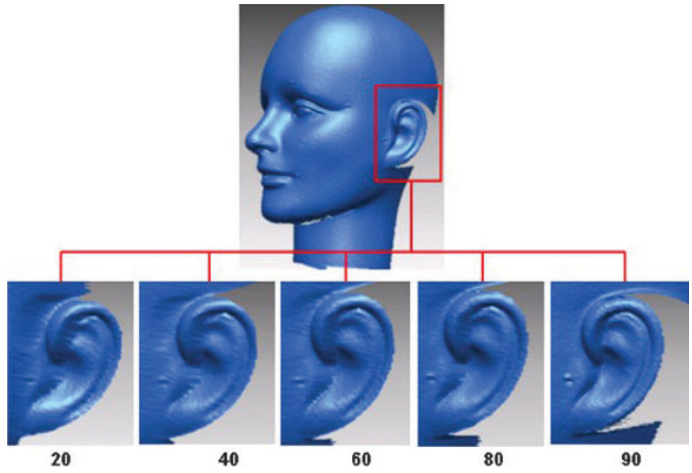

FIG. 17. Effect of the convergence angle to the modelled ear.

TABLE VIII. Slope distance comparison of the convergence angle test. Note that only the differences are presented.

From–To	$\alpha = 20°$ *(mm)*	$\alpha = 40°$ *(mm)*	$\alpha = 60°$ *(mm)*	$\alpha = 80°$ *(mm)*	$\alpha = 90°$ *(mm)*	$\alpha = 120°$ *(mm)*
3–8	−0·645	−0·747	−0·724	−0·532	−0·542	−0·297
4–9	−0·042	−0·474	0·107	0	−0·436	0·13
5–10	−0·431	−0·233	−0·636	0·251	0·619	−0·365
6–7	−0·82	−0·138	−0·384	−0·556	−0·017	−1·97
3–4	−0·035	−0·592	−0·472	−0·177	−0·197	−0·339
8–9	−0·571	−0·602	−0·213	−0·058	0·406	−0·024
2–11	−1·381	−1·361	−1·033	−1·433	−1·411	−1·514
Mean	−0·561	−0·592	−0·387	−0·358	−0·225	−0·626
Std deviation	0·433	0·371	0·276	0·514	0·621	0·736

loose correlation between the parameters. A study to find the mathematical correlation was not the objective of the research.

$$\sigma_{xyz} = (\alpha, I, N, f, S_d, R) \tag{1}$$

where

σ_{xyz} = 3D point standard error
α = convergence angle
I = laser beam intensity
N = number of scans per craniofacial area
f = focal length of the lens
S_d = scan distance, and
R = scan resolution.

Optimal Scan Distance and Camera Focal Length

Using a scan distance of 700 mm and the medium-angle lens has provided consistent accuracy for hundreds of scans of adult samples. However, it must be noted that the test results

were based on craniofacial areas of adult size. The craniofacial project in the future also calls for the mapping of infant samples. Consequently, more tests will have to be carried out on the much smaller craniofacial area of infants.

Laser Beam Intensity Test

As discussed elsewhere, higher beam intensity causes higher backscattering which appears as a blooming phenomenon. Subsequently, it was determined that the beam intensity has an adverse effect on the texture and accuracy of the captured 3D spatial data. A limited number of intensity values was selected for the comprehensive test (Table III). The reason was that a preliminary test based on 11 intensity values shows that the average shell–shell rms deviations—which satisfy the project accuracy requirement—were with the 20 to 40 bands. Nevertheless, no rigorous slope distance comparisons were carried out for these preliminary tests. Consequently, a comprehensive test for three intensity values (20, 100 and 150) was needed to confirm that the preliminary test result of using shell–shell deviation analysis was acceptable.

As a result of this test only the auto mode was used for the data capture and room lighting was maintained similar to that when the test was carried out.

Convergence Angle

With the limited number of convergence angles selected for the test it was difficult to pinpoint the optimal convergence angle within 5 degrees. The shell–shell deviation error size shows that a 90° angle gave the lowest average error (Fig. 15). Slope distance comparison showed the lowest mean was at 90° and the lowest standard deviation was at 60° (Table VIII). As both standard deviations satisfy the project requirement the lowest mean was selected as a better configuration. However, the texture and the shape for the ear were most comprehensible at 90°. This is an important feature for craniofacial mapping (Fig. 17). Based on the pixel size of 0·044 mm a difference of 0·073 mm in the standard deviation between 60° and 90° is obviously not large in terms of pixels. In other words, it is easy to miss 2 pixels in digitising the anthropometric mark. In addition, it is difficult to set the angle precisely for a regular hospital environment where patients' positions could be less than ideal. Consequently, it is believed a convergence angle of between 80° and 90° would be ideal.

Scan Resolution

It appears that the high and medium resolution scans produce similar measurement accuracy in this study. As mentioned elsewhere in the paper, the high resolution scan requires more time because it requires three repeated scans. Consequently, only the medium scan was used and thus far no error has been discovered in the work.

Live Face

Two other issues are worth a brief discussion: (1) facial hair and (2) facial movement. The scanner failed to capture data from facial areas which have a thick dark/black beard or a moustache. Generally, facial movement was not a problem with adult subjects. It became problematic when young children were involved as the left and right scans failed to merge accurately. As much as 25% of the work done on children required rescans.

CONCLUSIONS

Based on a preliminary study it was found that there could be a few important technical factors which could reduce the accuracy of captured laser scan data. Consequently, these factors were studied in more detail and the results show that accuracy could be degraded considerably. A more comprehensive study, though desirable, would have been significantly more time-consuming.

The findings show that the following parameters are optimal for the factors discussed:

(1) Scan distance: 700 mm ± 100 mm.
(2) Optimum lens: the medium-angle lens.
(3) Laser beam intensity: auto mode or set the value to between 20 and 40 at normal room lighting.
(4) Convergence angle: 60° to 90°—best at 90°.
(5) Scan resolution: medium resolution.

The mathematical correlation between the factors and the accuracy of the spatial data was not evaluated. Looking at equation (1), it is easy to see that the scale (S_d/f) is an important factor as well as the resolution (R). Other factors, such as laser intensity and the number of scans per craniofacial area, are rather flexible; the first is sensor-controlled and the second is limited by the number of scanners. The latter is an important factor for reducing facial movement during scanning, particularly of children. Also, dark or black facial hair is a problem. Tests carried out in various lighting conditions (from poor lighting to a brightly lit room) show that the scanner performs accurately in all conditions.

By and large, the study was useful because the knowledge gained was important in an endeavour to obtain high quality results. Based on the test results it was possible to achieve the project accuracy specification for the data captured.

Further research could include an intelligent system that automatically displays the achievable accuracy based on the lens used, the scan distance, the scan resolution and other necessary data.

ACKNOWLEDGEMENT

The authors acknowledge the support of the Ministry of Science, Technology and Innovation (MOSTI) Malaysia for the multi-million ringgit craniofacial reconstruction database project.

REFERENCES

ATKINSON, K. B. (Ed.), 1996. *Close Range Photogrammetry and Machine Vision*. Whittles, Caithness. 378 pages.

AUTODESSYS INC., 2004. Microscribe. 9 pages. http://support.knowlton.ohio-state.edu/files/MicroscribeFormz.pdf [Accessed: 27th June 2007].

BOEHNEN, C. and FLYNN, P., 2005. Accuracy of 3D scanning technologies in a face scanning scenario. *Fifth International Conference on 3-D Digital Imaging and Modelling*. 409 pages: 310–317.

BOYER, K. L. and KAK, A. C., 1987. Color-encoded structured light for rapid active ranging. *IEEE Transactions on Pattern Analysis and Machine Intelligence*, 9(1): 14–28.

DA SILVEIRA, A. C., DAW, J. L., KUSNOTO, B., EVANS, C. and COHEN, M., 2003. Craniofacial applications of three-dimensional laser surface scanning. *Journal of Craniofacial Surgery*, 14(4): 449–456.

FARAG, A. A. and EID, A., 2003. Video reconstructions in dentistry. *Orthodontics and Craniofacial Research*, 6(Suppl. 1): 108–116.

HAAR, F. B., CIGNONI, P., MIN, P. and VELTKAMP, R. C., 2005. A comparison of systems and tools for 3D scanning. 8 pages. http://vcg.isti.cnr.it/Publications/2005/TCMV05/WSH2005-24240.pdf [Accessed: 27th June 2007].

KAU, C. H., ZHUROV, A., SCHEER, R., BOUWMAN, S. and RICHMOND, S., 2004. The feasibility of measuring three-dimensional facial morphology in children. *Orthodontics and Craniofacial Research*, 7(4): 198–204.

KOVACS, L., ZIMMERMANN, A., BROCKMANN, G., BAURECHT, H., SCHWENZER-ZIMMERER, K., PAPADOPULOS, N. A., PAPADOPOULOS, M. A., SADER, R., BIEMER, E. and ZEILHOFER, H. F., 2006. Accuracy and precision of the three-dimensional assessment of the facial surface using a 3-D laser scanner. *IEEE Transactions on Medical Imaging*, 25(6): 742–754.

KUSNOTO, B. and EVANS, C. A., 2002. Reliability of a 3D surface laser scanner for orthodontic applications. *American Journal of Orthodontics and Dentofacial Orthopedics*, 122(4): 342–348.

MAJID, Z., SETAN, H. and CHONG, A., 2004. Modelling human faces with non-contact three dimensional digitizer—preliminary results. *Geoinformation Science Journal*, 4(1): 82–94.

MAJID, Z., CHONG, A. K., AHMAD, A., SETAN, H. and SAMSUDIN, A. R., 2005. Photogrammetry and 3D laser scanning as spatial data capture techniques for a national craniofacial database. *Photogrammetric Record*, 20(109): 48–68.

SANDERSON, A. C., WEISS, L. E. and NAYAR, S. K., 1988. Structured highlight inspection of specular surface. *IEEE Transactions on Pattern Analysis and Machine Intelligence*, 10(1): 44–55.

APPENDIX

TABLE AI. The true slope distance and slope measurements of the medium-angle lens measurement of various scan distances.

From–To	*True value*	$S_d = 700$ *mm*	$S_d = 800$ *mm*	$S_d = 900$ *mm*	$S_d = 1000$ *mm*
3–8	52·959	52·896	52·948	53·601	53·473
4–9	61·387	61·138	62·212	62·365	62·217
5–10	57·745	57·661	57·436	58·931	57·983
6–7	115·239	115·351	115·948	116·809	116·143
3–4	46·573	46·554	47·213	46·995	46·856
8–9	47·705	47·585	48·274	48·382	48·116
2–11	112·505	112·117	113·053	114·710	114·698

TABLE AII. The true slope distance and slope measurements of the wide-angle lens measurement of various scan distances.

From–To	*True value (A)*	$S_d = 700$ *mm*	$S_d = 800$ *mm*	$S_d = 900$ *mm*	$S_d = 1000$ *mm*
3–8	52·959	54·591	54·513	53·830	54·041
4–9	61·387	63·888	63·032	63·000	62·928
5–10	57·745	59·821	59·363	59·203	58·772
6–7	115·239	119·314	118·879	118·187	118·281
3–4	46·573	48·688	48·202	48·260	48·268
8–9	47·705	49·305	48·700	49·242	49·245
2–11	112·505	116·621	116·359	116·221	114·945

Résumé

L'intérêt des systèmes à balayage laser pour les relevés métriques cranio-faciaux de I'homme s'est considérablement accru dernièrement du fait qu'ils constituent des méthodes sans contact très efficaces pour saisir des quantités importantes de données localisées précises. Toutefois une évaluation complète est nécessaire pour identifier les principaux facteurs techniques qui peuvent oblitérer la précision de ces systèmes. On présente dans cet article les essais effectués avec le système de balayage à laser MINOLTA VI-910 à 3 D pour saisir des données de surface cranio-faciales, et les résultats de cette évaluation. L'étude a montré que les facteurs impliqués dans cette cartographic cranio-faciale étaient les suivants : la distance de l'objet balayé, la longueur focale de la caméra, l'intensité du faisceau laser, la résolution du balayage, l'angle de convergence et le nombre des balayages en recouvrement.

Zusammenfassung

Die Anwendung eines Laserscanningsystems zur Erfassung menschlicher Gesichtszüge hat großes Interesse hervorgerufen, da mit dieser berührungslosen Messmethode sehr effizient große Datenmengen hoher Genauigkeit erfasst werden können. Trotzdem muss zunächst eine durchgreifende Analyse durchgeführt werden, um die wichtigen technischen Faktoren zu erfassen, die die Genauigkeit des Systems beeinflussen können. Dieser Beitrag stellt dazu die Versuche und Ergebnisse eines Minolta VI-910 3D Laserscanningsystems vor, mit dem menschliche Gesichtsoberflächen erfasst worden sind. Folgende Faktoren sind demnach zu berücksichtigen: Scan-Entfernung, Brennweite der Kamera, Intensität des Laserstrahls, Scan-Auflösung, Konvergenzwinkel und Anzahl überlappender Scans.

Resumen

La utilización de sistemas de escáner láser para el cartografiado craneofacial en personas ha recibido mucha atención recientemente ya que es un método sin contacto muy eficiente para obtener una gran cantidad de datos espaciales exactos. Sin embargo, es necesario realizar una evaluación minuciosa para identificar los factores técnicos importantes que pueden afectar a la exactitud del sistema. Este artículo examina las pruebas y resultados de una evaluación del sistema de escáner láser tridimensional Minolta VI-910 en la obtención de datos de la superficie craneofacial. La investigación señala que los factores a considerar en el cartografiado craneofacial son: la distancia de escaneado, la distancia focal de la cámara, la intensidad del haz láser, la resolución de escaneado, el ángulo de convergencia y el número de escaneos con solape.

